

Design and Analysis of a Hybrid Vine Robot with a Mobile Joint System

A dissertation submitted to The University of Manchester for the degree of
Bachelor of Engineering in Mechatronic Engineering
in the Faculty of Science and Engineering

Year of submission

2025

Student ID

10824383

School of Engineering

Contents

Contents	2
List of figures	5
Abstract	7
Declaration of originality	8
Copyright statement	9
Acknowledgments	10
1 Introduction	11
1.1 Background	11
1.2 Motivation	12
1.3 Aims and objectives	13
2 Literature Review	14
2.1 Introduction	14
2.2 Disaster Robotics	14
2.3 Tracked & Crawler Robotics	15
2.4 Snake & Hyper-Redundant Robots	16
2.5 Tendon-Actuated Robots	17
2.6 Soft Robots	17
2.7 Vine Robots	18
2.8 Summary	20
3 Concept	21
3.1 Introduction	21
3.2 Methodology	21
3.3 Scenario Modelling	22
3.4 System requirements	23
3.5 Locomotion Analysis	24
3.6 Steering Analysis	25
3.7 Proposed System	26
3.8 Summary	28

4 Modelling	28
4.1 Introduction	28
4.2 Methodology	28
4.3 Operating Conditions	29
4.3.1 Eversion	29
4.3.2 Inversion	30
4.3.3 Stationary	30
4.4 Bending	31
4.5 Resistive	31
4.6 Reeling	32
4.6.1 Joint Movement	33
4.7 Workspace Analysis	33
4.7.1 Forward Kinematics	33
4.7.2 DH Parameters	34
4.7.3 Reachable Workspace	35
4.8 Summary	35
5 Design	36
5.1 Introduction	36
5.2 Methodology	36
5.3 Propulsion Design	36
5.4 Steering Design	37
5.4.1 Extension	38
5.4.2 Revolute	39
5.5 Gearbox Design	40
5.6 System assembly	40
5.7 Component Selection	41
5.8 Summary	41
6 Results	41
6.1 Introduction	41
6.2 Methodology	42
6.3 Path Length Dependency	42
6.4 Path Bend Dependency	43
6.5 System simulator	43

6.5.1 Block Diagram	43
6.5.2 Simulator	43
6.6 Summary	44
7 Discussion	44
8 Conclusion	45
References	45
Appendices	49
A Project outline	49
B Risk assessment	52
C Code	54

Word count: 1000

List of figures

1	Kosovo Security Force rescuers searching for survivors in the rubble of a collapsed building after the 2019 Albania earthquake (Ministry of Defense - Republic of Kosovo) [2]	11
2	"Robots used during the Chernobyl cleanup" by Wikimedia Commons [3] is licensed under CC BY 2.0.	15
3	An urban search and rescue robot moves across a rubble pile in a recent NIST/DHS exercise Credit: NIST[8]	16
4	SnakeBot in upright pose Credit: NASA[14]	17
5	(a) Diagram of vine robot base station, (b) Internal pressure pulls material released at base of the vine robot towards the tip causing eversion, (c) Vine robot shows significant increase in length due to pressure driven expansion	19
6	Main caption for all images	23
7	Diagram of different locomotion methods considered, sketched on remarkable.	24
8	(a) Proposed setup of mobile joint vine robot (b) Functionality of mobile joints (c) Vine robot approaches opening to a confined space (d) Vine robot everts pulling joints towards the tip and steering the most distal joint towards the victim (e) Material fed through joint 1 causing eversion at the tip and coalescing joint 2 into joint1 (f) Joint 1 moves to tip of vine robot steering tip towards the victim, joint 3 moves to coalesce with joint 2 preparing to take it's place (g) Material reeled through joint 1 causing eversion and joint 2 to coalesce with Joint 1 maintaining the bend and freeing up joint 1 to move towards the tip (h) Joint 1 moves to the tip and steers it in the direction of the victim (i) material is fed through the joints causing tip eversion and bringing the tip of the vine robot to the victim	27
9	Diagram illustrating forces on vine robot tip and the most distal mobile joint	29
10	Kinematics Diagram	34
11	Reachable Workspace	35
12	Spring Roller	37
13	Exploded view of locomotion module	37
14	Telescopic Actuator Cross section	38
15	Telescopic Gearing	39
16	Exploded view of extension module	39
17	Revolute Arm Length Analysis	39
18	Exploded view of Bending module	40

19	Path Length Dependency of Proposed Vine Robot and Base Reeling Vine Robot	42
20	Path Length Dependency of Proposed Vine Robot and Base Reeling Vine Robot	44

Abstract

This report presents a novel actuation method for vine robots that introduces shape-locking capabilities and enables path-length independent operation, provided that link bendage remains minimal. The proposed design enhances shape control compared to traditional reeling-based systems, offering improved adaptability in environments such as unstable structures or sparsely obstructed hazardous zones. While not well-suited for highly tortuous environments due to increased internal friction at high joint angles, the system demonstrates potential in controlled scenarios like industrial maintenance, where environmental geometry is known in advance. Despite limitations in experimental validation due to time, budget constraints, and organizational challenges—including a mid-project change in supervision—meaningful theoretical results were achieved, indicating the viability of the proposed system in specific real-world applications.

Declaration of originality

I hereby confirm that no portion of the work referred to in the thesis has been submitted in support of an application for another degree or qualification of this or any other university or other institute of learning.

Copyright statement

- i The author of this thesis (including any appendices and/or schedules to this thesis) owns certain copyright or related rights in it (the “Copyright”) and s/he has given The University of Manchester certain rights to use such Copyright, including for administrative purposes.
- ii Copies of this thesis, either in full or in extracts and whether in hard or electronic copy, may be made *only* in accordance with the Copyright, Designs and Patents Act 1988 (as amended) and regulations issued under it or, where appropriate, in accordance with licensing agreements which the University has from time to time. This page must form part of any such copies made.
- iii The ownership of certain Copyright, patents, designs, trademarks and other intellectual property (the “Intellectual Property”) and any reproductions of copyright works in the thesis, for example graphs and tables (“Reproductions”), which may be described in this thesis, may not be owned by the author and may be owned by third parties. Such Intellectual Property and Reproductions cannot and must not be made available for use without the prior written permission of the owner(s) of the relevant Intellectual Property and/or Reproductions.
- iv Further information on the conditions under which disclosure, publication and commercialisation of this thesis, the Copyright and any Intellectual Property and/or Reproductions described in it may take place is available in the University IP Policy (see <http://documents.manchester.ac.uk/DocuInfo.aspx?DocID=24420>), in any relevant Thesis restriction declarations deposited in the University Library, The University Library’s regulations (see <http://www.library.manchester.ac.uk/about/regulations/>) and in The University’s policy on Presentation of Theses.

Acknowledgments

I would like to acknowledge the guidance and support received from my supervising tutors: Dr Simon Watson, and Dr Ognjen Marjanovic.

I would also like to acknowledge the importance of the dedicated and detailed proof reading of Mary Prest

1 Introduction

1.1 Background

During natural disasters, such as earthquakes, landslides, or tsunamis, urban search and rescue (USAR), there is a vital response to minimize the death toll from these events. In the case of earthquakes, this involves surveying and excavating the rubble of collapsed buildings to locate and safely extract survivors [1]

During the aftermath of an earthquake, the challenge lies in locating survivors trapped under debris, who make up around 20% of survivors and include the majority of victims. Surveying and excavating the rubble of collapsed buildings is essential to ensure survivors can be found and extracted, as the fatality rate of survivors peaks after the first 48 hours[1]. This raises the importance of quickly locating survivors in collapsed structures for extraction or aid delivery.



Fig. 1. Kosovo Security Force rescuers searching for survivors in the rubble of a collapsed building after the 2019 Albania earthquake (Ministry of Defense - Republic of Kosovo) [2]

This is where disaster robotics plays a crucial role in USAR; assisting in rapidly identifying, evaluating, stabilizing, and evacuating individuals trapped in inaccessible locations. Disaster robotics focuses on developing and deploying robotic systems to enhance emergency response and recovery efforts in hazardous environments. These systems enhance human responders' capabilities by expanding their situational awareness and operational reach in challenging environments.

These robots also reduce human risk in disasters ranging from earthquakes to industrial incidents, assisting in tasks such as victim detection, structural inspection and adaptive shoring. The use of these robots can help enhance search efficiency and reduce risks to rescuers and the rescued.[1]. Existing approaches in Disaster USAR Robotics emphasises rigid robots designed for hazardous environments, focusing on mobility, manipulation and reliability. These rigid systems offer high precision and load capacity in addition to controlled manipulation for precise object handling. How-

ever, many of these rigid systems struggle with unstructured surfaces and unexpected obstacles, and their rigid nature can prove problematic for interacting safely with humans.

Soft robotics primarily mimics biological mechanisms (e.g., octopus tentacles, Muscles or earthworm locomotion) and is an emerging field of robotics with promising applications to Disaster Robotics is Soft Robotics,. By mimicking biological mechanisms, soft robots can perform delicate manipulation of debris, safely interact with survivors, and traverse uneven terrains while minimizing harm to both victims and responders.

These systems excel in confined spaces —such as collapsed buildings or rubble; leveraging compliant materials and adaptive designs to navigate complex, dynamic environments where traditional rigid robots struggle. Their inherent safety and flexibility make them ideal for collaborative human-robot teams in disaster zones, due to their ability to deform, squeeze through narrow gaps, and conform to irregular surfaces without causing further structural destabilization. However, soft robots are not perfect when compared to traditional rigid robots. Compromises include: reduced load capacity; limitations around accuracy in precision challenges; and requirements for greater power and control complexity.

The environments involved in disaster scenarios are generally confined spaces filled with rubble and debris which are non-uniform and potentially unstable. This is a great proving ground for soft robots. Debris often consists of sharp materials, such as broken glass, rock, and exposed metal and various other materials found in buildings such as carpets and slurries can occupy these spaces. This can pose risk to certain soft robots depending on their actuation mechanism, whilst others excel in resilience when compared to rigid robots.

Survivors who are not found during the initial stages of rapid search and rescue are usually trapped in void spaces within the rubble, which can vary in size. These confined spaces often lack ventilation, increasing the risk of suffocation due to the buildup of carbon dioxide. The pneumatic nature of soft robotics also offers exciting possible opportunities for fluid transfer as part of the robot's core mechanisms where this is already integrated.

1.2 Motivation

Traditional rigid robots face inherent limitations in USAR Environment, especially in the navigation of confined spaces as they often have limits on investigation depth and also present potential risk to structural stability.

The motivation for this project is to apply novel soft robotic systems to USAR Scenarios to advance the understanding of soft robots in this context as well as knowledge of soft-rigid body interactions.

Soft Robotics has the potential to revolutionise USAR, with its bio-inspired designs and innovative control strategies.

In practical applications soft robots can improve safety of humans during rescue operations. In addition, their compliance allows for better manipulation of delicate structures like rubble or debris as well as navigation of confined spaces or tight voids

By searching the small spaces in the rubble a robot can perform inspection without the need to excavate, which reduces time and labour spent in this process that can be used elsewhere. The use of these robots also minimises the exposure of rescue workers to hazardous conditions, improving the overall safety of the rescue efforts.

This Technology has the potential to contribute to other domains such as healthcare, pipe inspection or exploration in hazardous environments.

1.3 Aims and objectives

The Aim of this project is to identify challenges in the application of USAR robotics in tightly confined spaces

Objectives.

1. Conduct a literature review of preexisting USAR solutions, the problems they face and their applications
2. Construct a design specification to which preexisting and the solution discussed in this report can be appraised
3. Design a system overcoming the problems covered in the literature review
4. Test either physically or simulated for design validation
5. Evaluate validity of design considering written specifications

2 Literature Review

2.1 Introduction

Urban Search and Rescue (USAR) robotics addresses critical challenges in disaster response, where unstable terrains, confined spaces, and hazardous environments hinder traditional rescue efforts. Robotic systems mitigate risks to human responders while enabling access to areas compromised by collapsed structures or chemical contaminants.

This literature review aims to evaluate recent advancements in robotic designs and technologies that are specific or applicable to USAR applications. To identify gaps and opportunities for future research into disaster robotics.

Looking at the trade-off between mobility and control complexity; bio-inspired designs verses traditional mechanical approaches and the challenges with deploying these robots in real-world disaster scenarios, the following areas will be covered:

- Tracked and Crawler Robots for robust terrain navigation.
- Snake and Hyper-Redundant Robots for confined spaces.
- Soft Robots for adaptability in unpredictable environments.
- Vine Robots for growth-based exploration in narrow gaps.

In each of these sections we will look at different robot types, analysing their design principles, capabilities, limitations, and relevance to USAR tasks. All research included in this literature review was published post-2000 and has been published in peer-reviewed journals, sourced via online repositories. There were no geographic limitations placed on research origins. Key search terms included (but were not limited to): soft robotics, rescue robotics, disaster robotics.

2.2 Disaster Robotics

Within the field of disaster robotics, rescue robots have two general descriptors: ‘modality’ and ‘size’[1]. For the situation of navigating confined rubble, Unmanned Ground Vehicles (UGVs) tend to be the most suitable modality, due to their required operational space and mobility.

Robustness and Terrain Adaptability are very important for these robots as they need to be able to navigate through rubble, uneven surfaces and confined spaces without becoming inoperable or causing structural instability.



Fig. 2. "Robots used during the Chernobyl cleanup" by Wikimedia Commons [3] is licensed under CC BY 2.0.

These robots are also designed with human-robot Interaction in mind as most operators in these disaster scenarios will have had minimal training time with the robot, if any at all.

A restriction of navigating a robot through rubble is the need for teleoperation as the robot is inaccessible whilst in this environment.

The rubble, usually containing metal, renders wireless communication virtually inert[4]. For UGVs, this generally leaves the option of a tether or deployed repeaters which increase the operational range of wireless communications for the robot. Both options place constraints on the investigation depth of these robots, where the depth is further reduced by the complexity of the path taken.

2.3 Tracked & Crawler Robotics

The common practice for UGVs in general is polymorphic tracked vehicles. This can be seen in search and rescue robots such as the Soryu-IV[5] and MOIRA[6], which both feature modular designs with crawler sections to propel the robot forward through the rubble. Although, when compared to wheels tracks have a greater pulling force by 30% [7].

Coupled with the track's ability to adapt to different surface conditions of terrain, they seem quite suitable for rubble navigation. However, it has been shown that tracked robots are more susceptible to interference from their surface conditions as shown in the la Conchita mudslide where tracks were derailed by mud and shag-pile carpet[9],], although there have been developments to tracked robots since this event. The solution to this has been to use a combination of wheel and tracked robots such as Quince[10] or Atlas[11]



Fig. 3. An urban search and rescue robot moves across a rubble pile in a recent NIST/DHS exercise Credit: NIST[8]

Another limitation posed by crawler robots in collapsed rubble is the need for a tether, for recovery and communication. As propulsion to overcome the friction of the tether proportionally correlates to the size of the robot which limits the depth the rubble can be explored by these means. This can also be observed by the maximal widths of both MOIRA and soryu-IV with respective widths of 15 cm[6] & 160 mm[5].

Overall, these crawler robots show good mobility over rubble terrain as well as having good modularity, but are limited by their need for a tether and the size needed to actuate the treads and the postural change. This makes these robots more suitable for less confined spaces with irregular terrain.

2.4 Snake & Hyper-Redundant Robots

This leads us to our next promising area of interest, that of hyper-redundant snake robots. These robots are bio-inspired, mimicking the design of a snake, and possessing many degrees of freedom. This lends itself well to the navigation of collapsed rubble, as shown in Whitman (2018) [12] where a snake robot was successfully deployed in the aftermath of the 2017 Mexico city earthquake. There have been other successful designs of these snake robots, such as in Chavan (2015) [13]. Although this wasn't tested in a disaster site, it still demonstrates the ability to traverse collapsed terrain such as small gaps and pipes.

Snake and Hyper-redundant robots tend to have a smaller diameter than crawler robots. In addition to this, their locomotion methods can replicate the movement of tracked, crawling, and legged robots [12] allowing them to tailor their locomotion strategy to the current terrain. The options provided by these many degrees of freedom also allow for behaviours such as pole climbing which



Fig. 4. SnakeBot in upright pose Credit: NASA[14]

are exclusive to snake robots.

Despite the exciting movement principle they possess, these robots still pose the restriction of a tether which limits the robot to a predefined length that is affected by the complexity of the path the robot takes.

2.5 Tendon-Actuated Robots

Tendon-actuated robots present benefits similar to previously mentioned robots in terms of their ability to navigate complex terrains in USAR sites. They are typically lightweight and relatively inexpensive with diverse movement capability. They are particularly effective in terms of force application at a distance which enables them to reach situations where there are obstacles which cannot be traversed by other robots or human operators. One study [15] have raised concerns regarding reliability as fatigue failure in the tendon actuation wire would be a critical failure of the robot. This type of robot is also not suitable for miniaturisation.

2.6 Soft Robots

Another promising area for search and rescue robots in collapsed rubble is soft robots that can squeeze through small gaps.

Soft robots often mimic biological organisms like octopuses, worms, or starfish to achieve deformability, elasticity, and adaptive movement. This is achieved through the use of flexible materials (e.g., silicone, thermoplastic polyurethanes, hydrogels) that enable safe interactions and energy-efficient motion.

Previous USAR Robots such as Active-Hose [16] , a multi-segment hose like robot, that combined

soft features with rigid ones to augment the capabilities of the robot in USAR Scenarios. Active-Hose combined flexible bending joints with either pneumatic crawler joints or electric wheel joints to facilitate movement. This study tested both rigid and soft propelling units, and identified the soft propelling units more suitable to uneven terrain. This demonstrates how the compliance of soft robotics lends itself to USAR tasks.

North Carolina State University developed LEAP [17]], a lightweight and compact size soft robot, allowing access to confined spaces where larger robots or humans cannot reach. Bioinspired by the cheetahs high speed galloping, LEAP uses soft pneumatic bending actuators acting as muscles in conjunction with linkages acting as a ‘spine’ to replicate this gait. The robot’s gait allows it to climb steep inclines, a common challenge in disaster zones.

This design has also proved suitable for water-based search scenarios, when equipped with a fin.

This amphibious functionality could aid in flood related rescues or submerged disaster sites.

Although its soft elastic design reduces the risk of causing structural instability when interacting with unstable structures, it’s forceful galloping gait has the potential to destabilise fragile rubble during traversal. LEAP is also likely to struggle with communication reliability in disaster zones due to the lack of communication through collapsed rubble, and it’s small size doesn’t lend itself to overcoming the friction of being attached to a tether.

The Development of soft robot grippers such as OctArm[18], which uses a series of Octopus biology-inspired soft robot manipulators, overcomes the limitations of traditional rigid-linked robots by offering flexibility, adaptability, and dexterity.

The core of the OctArm design lies in its air muscle actuators, also known as McKibben actuators. allowing for smooth, continuous movements and the ability to conform to and grasp objects using whole arm manipulation.

Unlike rigid robots, OctArm shows adaptability in unstructured spaces due to its flexible nature. Demonstrating the ability to operate in both air and water, this suggests the potential for deployment in USAR scenarios, although it’s design complexity scales with length and number of segments and this does not lend itself well to deep exploration of USAR Scenarios.

However, OctArm lacks shape sensing which hinders operational accuracy and in some instances has caused grasp instability due to not being able to correctly perceive the robot’s shape.

2.7 Vine Robots

A promising field of soft robots for application in USAR Scenarios is Vine Robots. Vine Robots operate on the principle of transporting new material to the tip as a method of extension. The exten-

sion principle of vine robots is shown in Figure 6 where new material is unreeled in the base station of the vine robot and is transported towards the tip via a build-up of pressure within the vine robot body. As vine robots only grow new material at the tip their method of growth does not create friction forces with their environment friction is only occurs within the vine robots body. The lack of friction forces involved in growing a vine robot in an environment make it suitable to USAR deployment, as the environments of collapsed rubble are filled with loose debris and cause high friction when tethers are employed to maintain teleoperation of rescue robots.

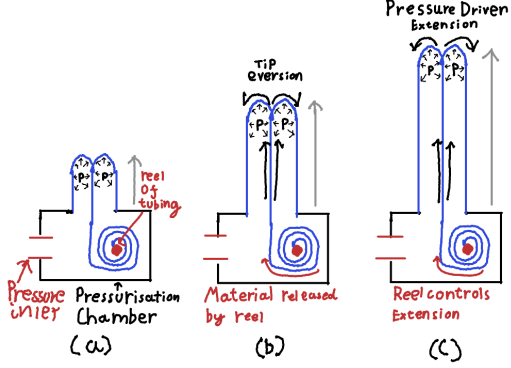


Fig. 5. (a) Diagram of vine robot base station, (b) Internal pressure pulls material released at base of the vine robot towards the tip causing eversion, (c) Vine robot shows significant increase in length due to pressure driven expansion

Some of these methods of vine robot actuation involve implementation across the whole length of the robot. One example of this is SPROUT [19] which uses 3 series pouch motor actuators spaced around the circumference of the body and attached along the length. The actuation of the body of the vine robot also causes scraping and friction, potentially causing damage to the robot and the sensor it carries. Due to the steering method being manufactured into the whole length of the robot, this can make the robot easier to fix if damage occurs in-site as if the sheath is damaged there is the possibility that the whole sheath will have to be replaced. This is beneficial in time critical situations with potentially untrained operators where damage may result in critical failure of the robot including the potential for it to be abandoned.

There have been various steering and retraction devices that use the concept of small hard robots situated at the tip of soft vine robots to enhance their manoeuvrability. These methods of vine robot actuation have low manufacturing complexity due to integration of these robots into the vine structure without having to manufacture anything additional into the length of the vine robot.

Past retraction work by Coad et al (2020) [20] implements a rigid reeling device placed within the vine robot's tip. This design improves on previous vine robots which exerted a reeling force from

the base instead of at the tip. As the reeling is done at the tip instead of the base, the frictional force of the inner sheath is minimised by effectively making the length of the material to retract almost 0. This contrasts to where it is retracted from a base reel where the frictional force of the inner sheath against the outer sheath along the length causes required reeling force to increase with length. RoBoa [21] is a good example, employing robots mounted on the interior of a vine robot. RoBoa makes use of a pneumatic robot located at the tip of the vine robot. Attached to the tip, this pneumatic robot stays at the front of the vine robot giving steering capabilities at the tip during growth. However, there is no retraction mechanism for this robot which proves to have limitations on greater operational depth.

Another example of this being Haggerty et al (2021) [22] where a solid revolute joint holds the reel of Vine Material near the tip of the sheath, instead of in the base. This overcomes previous limitations on vine robot length due to not having tether friction from base to tip of the vine robot, but from the joint to the tip of the robot instead. As this joint doesn't stray far from the tip, this means the robot can grow new material at the tip at constant pressure not depending on the current length of the vine body. This improves on the work by Coad et al (2020) [20] by adding additional steering capabilities to a internal retraction device, but also places limits on vine length due to the size of the reel of vine material being constrained within the vine robot sheath instead of in the base station where space is plentiful.

2.8 Summary

Various states of practice in USAR Robotics have been analysed, starting with more traditional rescue robots and progressing onto snake robots with latter focus on the growing field of Soft Robotics due to their compliance. Tracked robots have proved themselves in previous disaster sites and are the most widely used rescue robots. However, they rely on a tether which limits their exploration depth. The compliance of soft robotics makes these robots very suitable to the exploration of collapsed rubble, especially with vine robots as these minimise friction forces with their operating environment. However hyper-redundant snake robots have also proved very suitable for navigating such complex environment due to their novel locomotion method which can replicate various methods of movement. In unpredictable environments the adaptability of these snake robots proves highly preferable.

3 Concept

3.1 Introduction

In this conceptual design chapter, we will be creating a system for deployment in confined rubble. The constituent parts of this system will be evaluated separately, based on their effectiveness at the task they are trying to complete. The system will then be evaluated based on feasibility, scalability and total effectiveness for the exploration of collapsed rubble.

3.2 Methodology

We will start off by clearly defining the problem scope and the functional requirements for the robotic system. Using functional decomposition, we will break down these complex tasks into sub-tasks which are then put into specification matrices to weight them due to their importance to the parent task they are trying to solve.

The potential solutions to these separate functional requirements will be generated with methods such as brainstorming, in addition to drawing from previous work in the field of USAR Robotics. There will be a focus on bioinspired design for soft robots and novel locomotion mechanisms. To evaluate the fulfilment of these technical requirements, the generated concepts will undergo matrix analysis (see below) to provide an unbiased view on their competency of fulfilling these requirements. The weighting of these matrices is shown in Table 1

Scale	Fulfillement	Criteria
1	poorly meets the criteria	has minimal impact
2	Meets the criteria to a limited extent	has some influence but not a major factor
3	Meets the criteria adequately	has a noticeable impact on the decision
4	meets the criteria well	significantly influences the decision
5	exceptionally fulfills the criteria	criteria is crucial and has the highest impact on the decision

Table 1. Analysis Weighting

The proposed system will be evaluated in a similar way but with different criteria as we then want

to look at the feasibility of the system

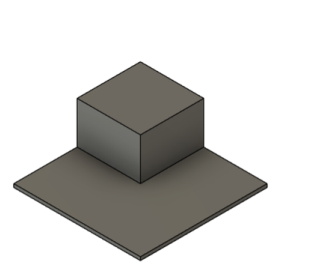
3.3 Scenario Modelling

The interior of a collapsed debris field is highly irregular and complex. To better assess the design within the scope of the project simplifications and abstractions of the environment have been made. Drawing on the development of Proboscis [23], where work was done in close conjunction with swiss rescue about constraints in collapsed rubble, this allows the definition of specific goals that can be integrated into a testing track to test the validity of the final design

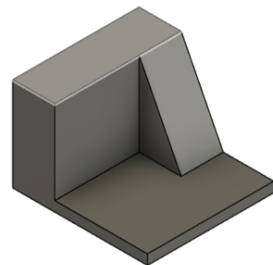
The testing track consists of the following 6 obstacles

- Unguided Turn - A solid block is located at one corner of the platform, this restricts the movement. the goal is to navigate around this block without any guidance. the steering system needs to have enough traction to prevent drifting away from the desired destination maintaining a radius of curvature less than 25 cm
- Height & Slope - the slope has a incline of 60 degrees with a step height of 50 cm.
- Gap - a trench has been cut out of solid material. the results of this test verify whether the system is able to navigate over an unsupported divide of 50 cm in width.
- Unguided Navigation - this obstacle simulates having to navigate through any large voids which may be present in the rubble, as there can be large open spaces.
- Obstacle Deviation - the result of this test verifies if the system can successfully navigate past an obstacle that is obscuring its path
- Guided Movement with spatial restrictions - this task represents navigating through a pipe network or around a system of corners

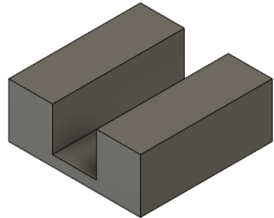
Compiling these requirements into a tabular matrix gives Table 2



(a) Unguided Turn



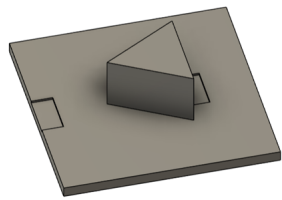
(b) Height & slope



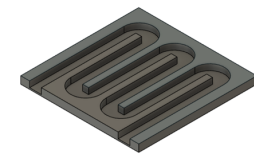
(c) Gap



(d) Unguided Navigation



(e) Obstacle Deviation



(f) Guided Movement with Spatial Restrictions

Fig. 6. Main caption for all images

Length	>	15m
Weight	<	50kg
Maximal Width	<	15cm
Max Bending Radius	<	25cm
Drive Direction	Forwards and Backwards	
Max Velocity	>	0.1 ms-1
Climbable Inclination Angle	>	45 degrees
Bridgable Gap width	>	50cm
Climbable Step Height	>	50cm
Supply	water	
Sensor	camera/lidar	

Table 2. System Requirements

3.4 System requirements

From the outcome of Sections [2],[3.3] the following system requirements are determined

- steering
- locomotion
- Minimising Friction

3.5 Locomotion Analysis

When considering the requirements on locomotion, this was decomposed into a series of sub-requirements to characterise their relevance to locomotion in collapsed rubble of USAR Scenarios. These can be seen as part of the analysis shown in Table 3 (below). Due to the nature of the inspection of confined rubble it is important to consider how the system interacts with the loose terrain and confined spaces. This creates a need to overcome uneven terrain and the friction that is generated by its tether, as wireless communication doesn't work in the rubble [1].

The different principles of locomotion that could be utilised by the robot the following options were brainstormed drawing on previous research in USAR Robotics. This is shown in Figure ??

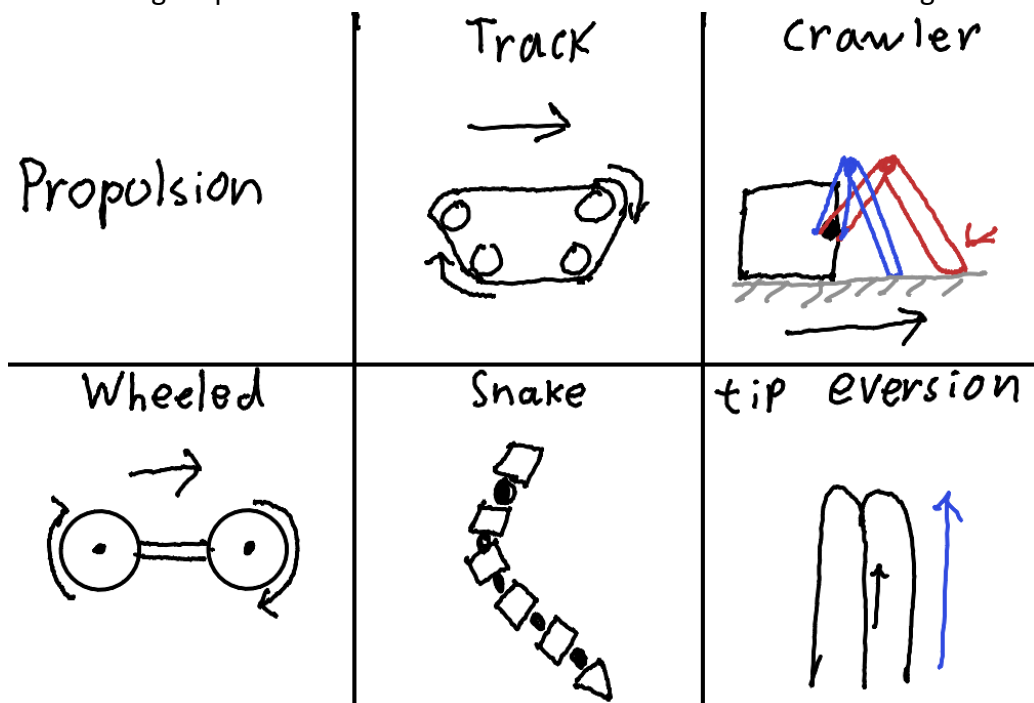


Fig. 7. Diagram of different locomotion methods considered, sketched on remarkable.

These different locomotion concepts are then analysed in Table 3 to impartially identify the most suitable option for USAR operation in collapsed rubble.

Comparison Metric	Weighting	Track	Crawler	Wheeled	Snake	Tip Eversion
Overcoming Obstacles	4	3	3	3	4	2
Overcoming Friction	5	3	3	4	3	5
Loose Terrain	5	4	1	2	4	5
Speed	1	4	2	4	2	3
Control Ease	2	4	3	5	1	2
Power Consumption	3	3	3	3	3	3
Total = sum(score x weighting)	68	42	65	64	74	

Table 3. Locomotion Analysis

As result of the analysis in Table 3 Tip Eversion is to be selected as the locomotion principle for the system. This is primary due to the properties of having no friction with its environment which allows the tether to be contained within a vine robot where the friction can be controlled. This feature of vine robots solves our requirement for minimising friction, which is vital in USAR Scenarios.

3.6 Steering Analysis

When considering the requirements of steering with our selected method of propulsion, we generate a set of sub-requirements through functional decomposition. These are set out and weighted due to their operational relevance in Table 4 . There are two main schools of vine robot actuation. These are largely separated by where this actuation occurs; either originating from the base of the vine robot or occurring elsewhere along the body, usually close to the everting tip of the vine robot. Base location has higher manufacturing complexity as it has to be preset into the whole length of the vine robot. This is not suitable for USAR as rescue robots need to be easily fixed or components easily replaced when failure occurs in the field. This consideration leads us to look at vine robot steering methods that have low manufacturing complexity with most of these methods being tip-based actuation.

Comparison Metric	Weighting	Solid Joints	Manufactured Bends	Constant Curvature	Tendon Actuated
Shape Locking	4	4	5	3	3
Steering Control	3	5	5	2	4
Manufacturing Ease	5	4	2	2	4
Exploration Depth	5	54	2	3	3
Adaptability	5	4	1	3	3
Total = sum(score x weighting)	96	60	58	74	

Table 4. Steering Analysis

Subjecting these steering concepts to matrix analysis gives use Table 4 where revolute joints are determined to be the most suitable option.

3.7 Proposed System

Integrating our chosen steering and locomotion concepts, the following system is proposed (see Figure 8). Implementing a series of rigid bending joints attached to the inner sheath of the vine robot, the proposed design aims to improve on previous hybrid-vine robot designs. These rigid joints consist of a revolute bending mechanism, enabling bending of the rigid joint, and a series of rollers, aiming to move the joint relative to the inner sheath of the robot. The mobile joints possess the ability to move along the length of the vine robot, providing a level of reconfigurable shape locking. By deploying bending joints at varying points along the vine length, this enables greater control of the shape of the vine body. Additionally, by implementing a reeling joint at the tip of the robot, this serves to aid in the function of retraction as shown in previous retraction work [22], [20]. This design aims to improve the operational capabilities of the vine robot, providing more control and configurability of the shape of the vine body. The design not only benefits the inspection of collapsed rubble, but can also lend itself to industrial inspection in situations such as pipe inspection.

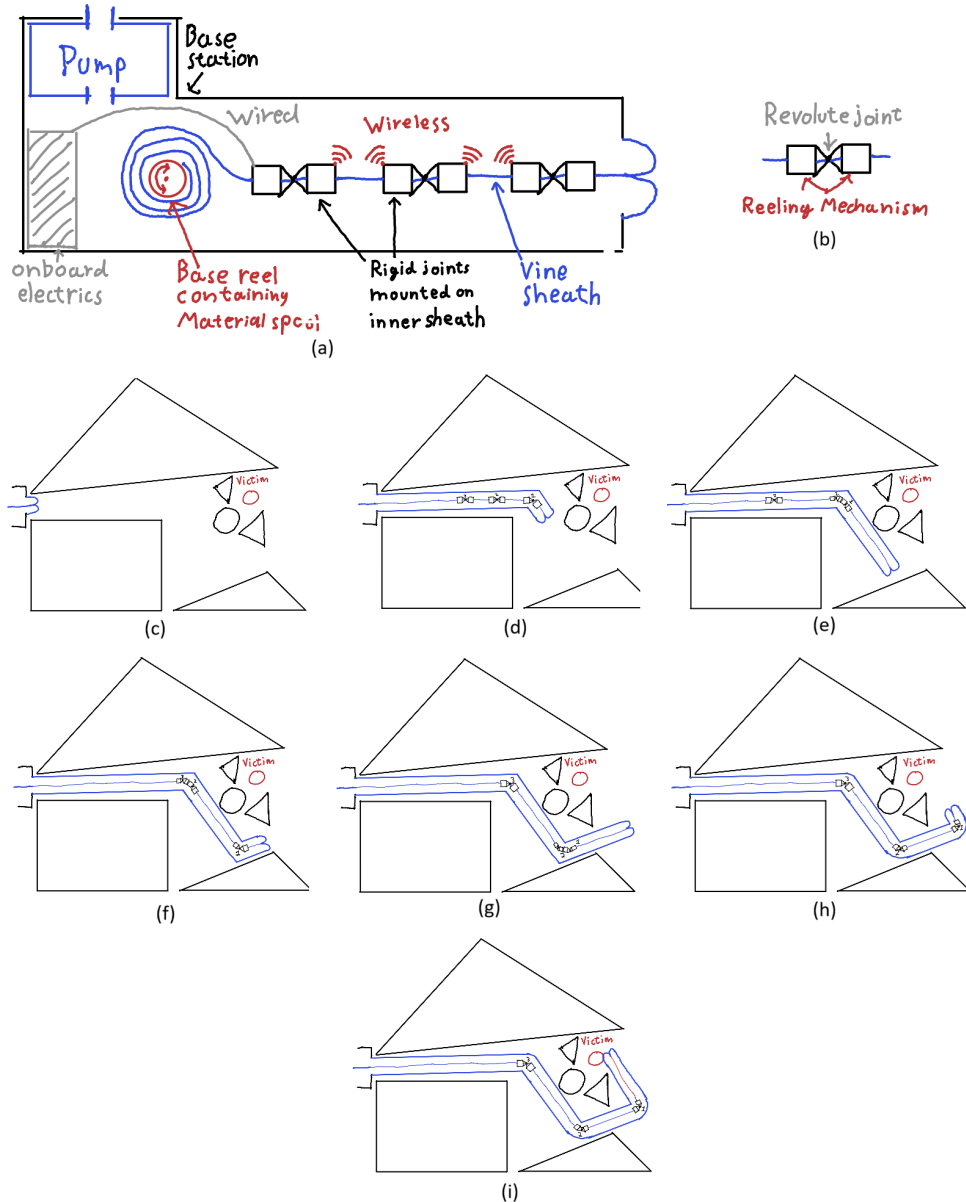


Fig. 8. (a) Proposed setup of mobile joint vine robot (b) Functionality of mobile joints (c) Vine robot approaches opening to a confined space (d) Vine robot everts pulling joints towards the tip and steering the most distal joint towards the victim (e) Material fed through joint 1 causing eversion at the tip and coalescing joint 2 into joint1 (f) Joint 1 moves to tip of vine robot steering tip towards the victim, joint 3 moves to coalesce with joint 2 preparing to take it's place (g) Material reeled through joint 1 causing eversion and joint 2 to coalesce with Joint 1 maintaining the bend and freeing up joint 1 to move towards the tip (h) Joint 1 moves to the tip and steers it in the direction of the victim (i) material is fed through the joints causing tip eversion and bringing the tip of the vine robot to the victim

Figure 8 also shows the theoretical operation of this robot configuration. where joints repeatedly coalesce and separate as they move along the length of the robot, in order to create various set bends based on the environment. When joints move through created bends towards the tip of the robot, multiple joints coalesce into collaborative units to facilitate the movement forwards. Acting as one, these joints contribute to the bend of the vine body. In each instance / change of direction,

after the individual joints coalesce we see the most distal of these two joints proceed further along the body and the previous joint replaces it, locking the shape of the vine body. On the return journey, the same would happen in reverse.

3.8 Summary

Overall, the proposed system builds on previous hybrid-vine robot research employing a mobile joint system that enhances the dexterity of the vine robot. This builds on previous research by adding a level of shape-locking into the hybrid vine robot which makes it suitable for operation in unstable structures where haphazard movement can cause structural instability.

4 Modelling

4.1 Introduction

In this Modelling Chapter, there will be characterisation of the robot and its operating environment to characterise the physical system. We then identify the key resistive forces and go on to mathematically characterise these to analyse the robots operating conditions. All of this feeds into creating a forwards and inverse kinematic model of the robot.

4.2 Methodology

Beginning with the definition of the operating environment, we will clearly describe the internal conditions that dictate the behaviour of the robot and specify relevant factors that may impact this.

This leads into the identification of key resistive forces which is analysed using a free body diagram to determine the forces on the system and illustrate their points of application.

Feeding into Mathematical Characterisation where presented empirical models represent each resistive force. Improving the accuracy of our generated kinematic model, and defining the operating conditions for the proposed robot.

4.3 Operating Conditions

First we will look at the operating conditions of the vine robot which dictate growth and the length of the robot

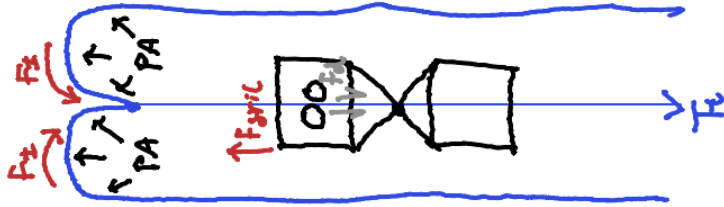


Fig. 9. Diagram illustrating forces on vine robot tip and the most distal mobile joint

4.3.1 Eversion

From modifying past work on the operating conditions of Hybrid-Vine robots [22], accounting for tail tension and the collective friction force of all the joints we get Equation (1)

$$\frac{PA}{2} > F_{fric} + F_i + T_t \quad (1)$$

Where $\frac{PA}{2}$ is the pressurisation force of the robot acting as tail tension to the tip at the most distal joint. F_{fric} is the resistive friction force of the robot joints against the outer sheath of the vine robot. F_i is a material constant of the material that opposes either inversion or eversion depending on what is trying to be achieved. T_t represents the tail tension before the most distal joint, representing the pulling force of the base reel.

In this case the pressurisation force acting at the tip PA exceeds the sum of the resistive forces pulling against it. once $\frac{PA}{2}$ has exceeded this boundary, material is pulled from the base towards the tip extending the length of the vine robot.

If we consider only the most distal joint of the system, setting F_{fric} to only represent the friction of this one joint, we can then further simplify this equation by setting $T_t = 0$. This is done by introducing slack between the most distal joint and the one that precedes it. By doing this we can simplify the conditions for eversion by disregarding all of the previous joint, aslong as $\frac{PA}{2}$ does not exceed $F_{fric} + F_i$ then there will be no eversion. This method requires tighter control of pressure but achieves more accurate control of vine length.

As T_t is present in Equation (1), although we have simplified this by setting $T_t = 0$, it is also possible to vary the value of T_t to vary the boundary conditions of the robot potentially causing change of length without introducing a change in pressure.

4.3.2 Inversion

Yet again modifying the equations from [22], including terms for our tail tension we obtain Equation (2)

$$\frac{PA}{2} < F_{\text{fric}} - F_i + T_t \quad (2)$$

Where all symbols have the same meaning as Equation (1).

In this case, as $\frac{PA}{2}$ is insufficient, the most distal joint is capable of reeling material from the tip. To account for the slack that is being created by the reeling of the most distal joints, all other joints including the base reel can also operate at the same time to ensure the inner sheath is taut.

4.3.3 Stationary

[22] also offers insights on conditions for joint movement within the sheath, we yet again modify this to include tail tension of the robot giving Equation (3).

$$F_{\text{fric}} - F_i + T_t < \frac{PA}{2} < F_{\text{fric}} + F_i + T_t \quad (3)$$

All symbols in Equation (3) have the same meaning as Equation (1). In this condition where $\frac{PA}{2}$ is within $\pm F_i$ of $F_{\text{fric}} + T_t$, the joints are capable of reeling themselves within the length of the vine robot. The forces produced by this movement may produce changes in the value of T_t . If this changes the boundary conditions and subsequently causes inversion or eversion, most likely inversion due to the increase of T_t , this subsequently alters the volume of the vine robot changing the pressure in accordance with the ideal gas equation Equation (4) given in [24].

$$PV = nRT \quad (4)$$

This means that there will be minimal length change during the movement of the joints, and that once the joints have finished movement and T_t returns back to the value it was before joint movement, that the length of the vine robot will also be the same.

4.4 Bending

Past work , gives us Equation (5) for the restoring moment of a inflatable beam under transverse loading

$$M_{\text{int}} = \pi \times P \times r^3 \quad (5)$$

where M_{int} is the moment produced by the deflected beam, P is the inflation pressure & r is the radius of the vine body. As Equation (5) is independent of angle of deflection this directly feeds into the torque requirements for our bending motors. As this moment does not vary across the length of the robot, each of our bending motors can have the same torque aslong as they exceed the value of M_{int} .

4.5 Resistive

Depending of the bend of our joints the frictional forces that these joints exert can also change, with a straight joint having a lower frictional force and a bent joint exerting a higher frictional force. This is due to an additional normal force exerted from the joint pressing into the side of the outer sheath. Modifying the Coulomb Friction equation in [25] to account for moments we get Equation (6) involving the normal force

$$M = \mu N r \quad (6)$$

where M is the moment exerted on the joint, μ is the coefficient of friction between the sheath and the joint & r is the radial distance from the joints point of contact with the sheath and the centre of the revolute joint.

Rearranging for N we get Equation (7)

$$N = \frac{M_{\text{int}}}{\mu r} \quad (7)$$

Which is then used to obtain Equation (8) for the joint friction force whilst bending. Assuming $|\theta_i| > \theta_{\min}$ where θ_i is the angle of bend of the i th joint and θ_{\min} is the minimum angle of joint bend for the joint to contect the sides of the outer sheath as $\text{JointDiameter} < \text{SheathDiameter}$.

$$F_{\text{fric}} = \mu(mg + N) \quad (8)$$

Assuming no bends in the vine sections between the joints then this equation is used to calculate

the friction forces of the joints. where total frictional force is given as

$$F_{\text{fric}} = \sum_{i=1}^n \mu(mg + Nf(\theta_i)), \quad f(\theta_i) = \begin{cases} 1 & \text{if } |\theta_i| > \theta_{\min}, \\ 0 & \text{otherwise.} \end{cases} \quad (9)$$

If there are additional bends between the joints due to obstacle deflection, this causes the inner sheath to become in contact with the outer sheath due to it not being supported by a rigid joint. This introduces another resistive force into the internal of the vine robot which increases exponentially with total curvature of contact. This is modelled as capstan friction in vine robots, shown in [26] where the path dependent resistive forces of a base reeling vine robot are characterised. Capstan friction being dependent on curvature is shown in Equation (10).

$$F_{\text{bend}} = \sum_i C e^{\mu_c \phi_i}, \quad (10)$$

where C is the configuration tension, μ_c is the coefficient of friction between the inner sheath and the outer sheath & ϕ_i is the angle of the i th bend that the cord is in contact with

The other path dependent force for

$$F_{\text{length}} = \mu_s w L \quad (11)$$

Where w is the normal force exerted per unit length, L is the length of the soft robot path & μ_s is the length dependent friction coefficient. The force F_{length} represents the normal friction force exerted by the weight of the inner sheath against the bottom of the vine body.

The effects of capstan friction can be managed in the proposed system by using the joints on either side of this deflection bend to reduce tension C in order to minimise the effects of capstan friction within the vine bot. As the inner sheath in the the mobile joint vine robot is suspended inbetween the joints and doesnt touch the bottom of the vine body, this eliminates the length-dependent normal friction force entirely, aslong as slack isn't introduced into the system.

4.6 Reeling

Previous work on retraction of vine robots [20] shows that the force required to invert a vine robot is equal to the pressurisation force plus the inversion/eversion force that resists this change in the vine robot length. Modifying this to include the friction between the vine body and the rigid joints gives

$$F_r \leq \frac{PA}{2} + F_i + F_{fric} \quad (12)$$

where P is the internal pressure, A is the cross sectional area of the vine robot, F_i is the material constant inversion/eversion force & F_{fric} is the friction force of the most distal joint. This Equation Assumes we only attempt inversion using the most distal joint of the vine robot. This can derive our maximum required reeling force for inversion where.

$$F_{rmax} = P_{max}A + F_i + F_{fric} \quad (13)$$

Inversion can also be implemented from the base reel, although this less suitable due to the higher friction force of all the joints and the drop in tension across the vine robot due to capstan friction.

4.6.1 Joint Movement

For the movement of joint within the vine robot body the reeling force of the rigid joint must exceed the frictional force it exerts in contact with the outer sheath.

$$F_r > F_f \quad (14)$$

This in turn alters that value of T_t in the inner sheath of the vine body. This shoudl have minimal effect to the overall vine length aslong as the pressure is sufficiently high to prevent inversion

4.7 Workspace Analysis

4.7.1 Forward Kinematics

Model assumes no deflection from obstacles The kinematics of the proposed system acts as a P n(RP) planar rigid robot where $n = No\ of\ Joints$ Williams and Shelley [27] provide the kinematics for this class of planar manipulators. Adapting this to our model gives Equation (15)

$$E = \begin{bmatrix} x \\ y \end{bmatrix} = A + L_0e^{j\theta_0} + L_1e^{j\theta_1} + \dots + L_n e^{j\theta_n}, \quad (15)$$

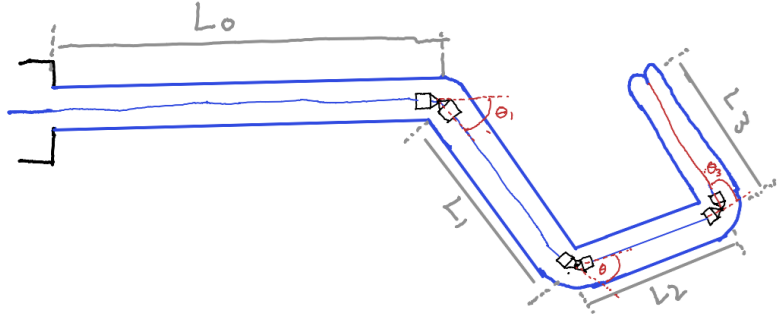


Fig. 10. Kinematics Diagram

Where (x, y) represent the global frame position of the end effector, A represents the global position offset from the placement of the base station, L_i corresponds to the length of the i th segment & θ_i is the orientation in the i th frame. The implementation of these values when $n = 3$ is shown in Figure 10.

This system has been zero indexed as θ_0 represents the orientation of the L_0 link, θ_0 will be equal to 0 aslong as there are no obstaces in the workspace that cause deviation in this linkage. $\phi = \theta_0 + \theta_1 + \dots + \theta_i$ gives the tip orientation in relation to the base frame, giving us our angle of approach. the values of θ_i & L_i are illustrated in Figure ???. The segment lengths are subject to the constraints shown in Equation (16).

$$L = \sum_{i=1}^n L_i, \quad L \leq L_{max}, \quad L_i \geq \text{Joint Length} \quad (16)$$

The constraints on L_i are due to the fact that the rigid Joints exert length beyond their axis of turning which imposes a minimum length on these link lengths

4.7.2 DH Parameters

Modelling this robot as a rigid plane manipulator we can also develop a set of DH Parameters for this robot. Given theat the robot is planar, this means that there is no link twist or link offset in the robot. Meaning all values for α & a are equal to 0 with $n = 3$ we get the following DH Parameters for or PRRPRRP Manipulator with θ_i corresponding to the angular positon of the bending motor of the joints, δ_i corresponding to the rotational displacement of the reeling motors, with δ_0 corresponding to the reeling motor in base reel & $\delta_1 \ \delta_2 \ \delta_3$ representing the rotational displacement of the reeling motors in the rigid joints. This model has limitation for accurate simulation, as it does not incorporate the soft properties of the vine body. This does not account for link bending and obstacle

joint no	Joint Typed	θ	A	alpha
1	P	$\delta_0 R + \delta_1 r + \text{offset} * 3$	0	0
2	R	0	θ_1	0
3	P	$\delta_0 R + \delta_2 r + \text{offset} * 2$	0	0
4	R	0	θ_2	0
5	P	$\delta_0 R + \delta_3 r + \text{offset} * 1$	0	0
6	R	0	θ_3	0
7	P	$\delta_0 R - \sum_{i=1}^{n-1} L_i$	0	0

Table 5. DH Parameters of a 3 joint vine robot with a mobile joint system

deflection

4.7.3 Reachable Workspace

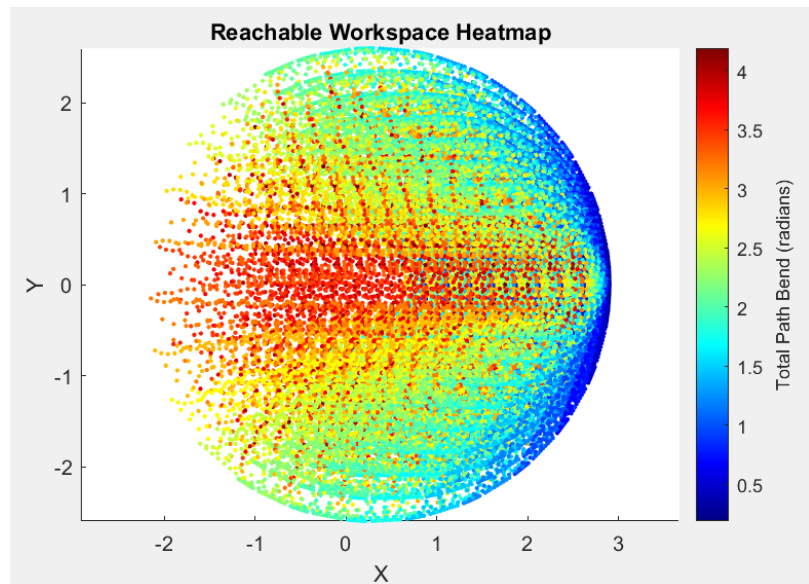


Fig. 11. Reachable Workspace

Figure 11 shows the reachable workspace of a mobile joint vine robot with a maximum length of 3m. This is plotted as a heatmap to display the angle of approach to get to each plotted point from the origin (0, 0) with the vine robot base aligned with the positive x-axis.

4.8 Summary

The mathematical characterisation of the proposed robot indicates that the mobile joint system does not have path length dependency and Capstan friction is not introduced into the system as long as the number of bends does not exceed the number of joints. In addition, it has been demonstrated that for eversion conditions, only the most distal joint needs to be considered, due to the

fact that tail tension can be reduced to ON by feeding any slack into the inner sheath before the most distal joint, rendering joint friction of other joints irrelevant, in relation to the tip. It is important to consider that this model does not account for obstacle deflection and deformation of the vine robot body. Instead, it simulates the proposed robot as a rigid planar manipulator, using an ideal kinematic scenario for analysis of deflection. Although this fails to measure the body distortion of the robot and its soft behaviour, it is important for understanding the shape of the vine body in the workspace.

5 Design

5.1 Introduction

The design process details the transition from conceptual design to detailed CAD work, taking input from the modelling section to inform component selection. Ensuring that the force requirements are met and that the design allows for easy assembly, manufacturing, access of individual parts and integration into the vine sheath

5.2 Methodology

There are a range of critical requirements derived from the modelling chapter including constraints such as weight, size, cost & manufacturing limitations which would inform the design process. Due to the constraints of the project, it has not been possible to analyse all of these elements. There has been a focus on consideration for manufacturing ease, force requirements and component sizing.

5.3 Propulsion Design

Due to not being able to experimentally obtain data of the vine robot within the scope of the project, the following design in Figure 12 is proposed. This sketch shows the design with spring actuated to account for different materials due to the material properties being unknown so normal force can be tuned. This design employs both a driven roller and a passive roller, where the driven roller is fixed and the passive roller is mobile put pushed towards the active roller by a compression spring.

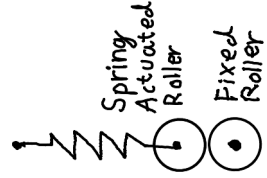


Fig. 12. Spring Roller

As the friction force between the roller and the sheath depends on the normal force between them, a spring is implemented in order to add tunability and adaptability to the roller. By reducing the space occupied by the spring, this allows for the force exerted by the spring to be modified by placing spacers in the spring housing. This proposed set-up is also capable of dealing with kinks in the inner sheath due to the movement of a passive roller.

This implementation of this design is shown in Figure exploded view. Due to the possibility of 3D printing the gearbox housing is merged into the body of the reeling mechanism to allow for efficient force transfer. The implementation of this design is shown in Figure 13 Exploded View. Due to the possibility of 3D printing the gearbox housing is merged into the body of the reeling mechanism to allow for efficient force transfer. exploded diagram explaining parts.

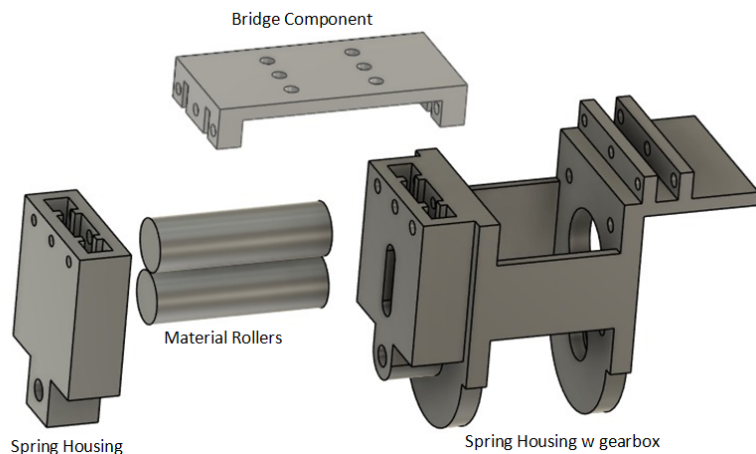


Fig. 13. Exploded view of locomotion module

5.4 Steering Design

Steering design needs to have sufficient length to exert bending moment on vine body yet needs to be small enough to transition through a joint to move towards the tip of the vine robot. This problem was solved by creating an extension mechanism so the joints are able to lengthen to exert this

bending moment and then subsequently be able to retract this added length so they are mobile enough to move through the bends of the vine body

5.4.1 Extension

in order to extend the length of the rigid joints multiple times their own length a telescopic actuator was implemented using the design in Figure?? cross sectional diagram for telescopic screw actuator The proposed design is a two stage telescopic actuator that allows the rigid joint to increase it's length by up to 300% to ensure even extension, these telescopic actuators are situated on op-

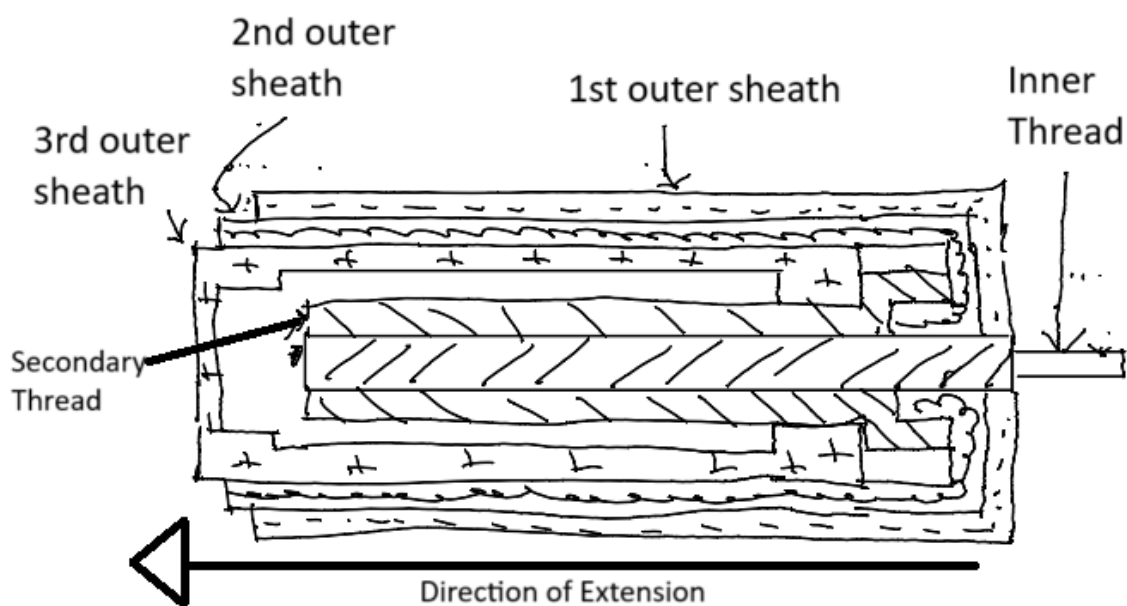


Fig. 14. Telescopic Actuator Cross section

posite sides of the vine robots circumference. it is possible to actuate both of these screwed telescopic actuators with a geared chain, but due to the possibility of obstructing the inner sheath of the vine robot passing through the joint this was deemed to not be a valid option instead a modified version of a planetary gear was used. diagram for ring with propulsion design specifying diameter of the ring diagram for actuator of inner rotary ring this design is laid out in Figure 15 diagram for ring with propulsion design specifying diameter of the ring diagram for actuator of inner rotary ring this design makes use of a internal spur gear mounted on the interior of a large bearing. where the inside of the bearing is free to rotate and the rest of the joint components mount to the outer ring of the bearing. The gearbox to drive this mechanism was also merged with the body of the outer ring bearing to ensure efficient and accurate force transfer to the intermediate gear This final design is shown in Figure Exploded diagram. exploded diagram showing parts for this assem-

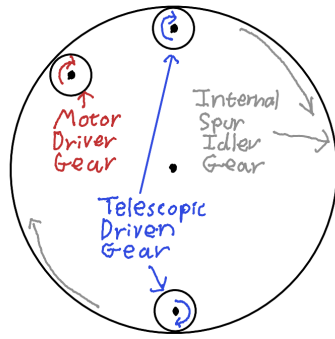


Fig. 15. Telescopic Gearing

bly

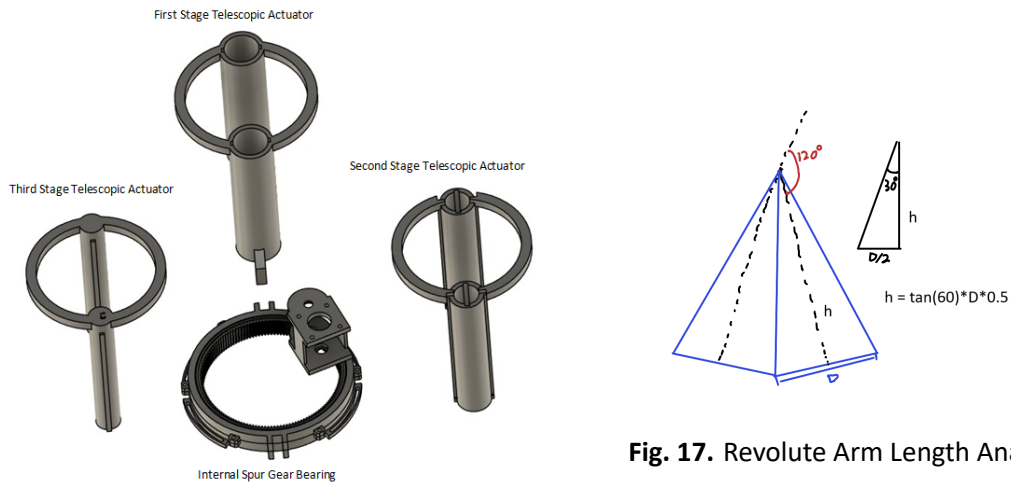


Fig. 17. Revolute Arm Length Analysis

Fig. 16. Exploded view of extension module

5.4.2 Revolute

consistent with previous work on Internal steering mechanism of vine robots, the maximum joint bend was set to 120° . The derivation process for the revolute joint arms to connect both sections of the extension mechanism together is illustrated in Figure 17

This design was split into an inner and outer arm to allow for full rotation and ease of assembly where the Gearbox was merged with the body the full implementation of this is shown in Figure 18 showing arm length limiting turning to 120° exploded diagram showing parts for assembly and motor placement

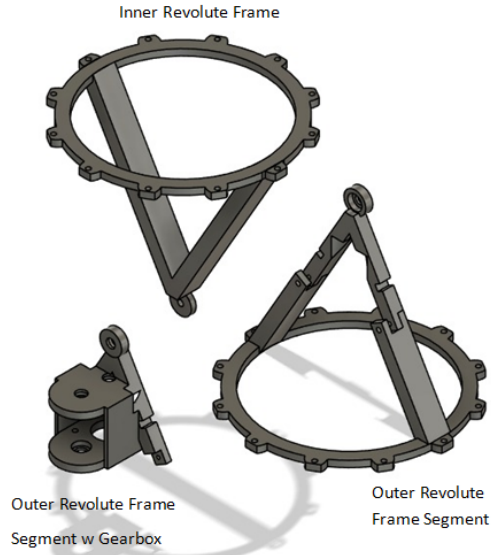


Fig. 18. Exploded view of Bending module

5.5 Gearbox Design

as the design of the rigid joint doubles the diameter of the joint used in [22] and we also know due to (5) that the restoring moment scales with r^3 , this incurs a 8 times increase to the required bending force characterised in the previous hybrid steering work. to overcome this a 3 stage gearbox was used. As the only stepper motors in our budget have an output torque of 0.2 Nm, a factor of 4 was used for each stage of the gearbox. assuming 90 % efficiency for each stage of the gearbox our new torque is given as

$$T_{out} = T_{in}(\text{Gear Factor} * 90\%)^3 \quad (17)$$

using Equation (17) with the value of $T_{in} = 0.2Nm$ and each gear factor to equal 4 we predict the output torque to be around 9.3N. The actual value may be lower than this due to the real gear system being more inefficient than expected.

5.6 System assembly

diagram showing complete system highlighting points of attachemet and materials used assembling the whole system into the rigid joint gives Figure Complete Joint View

5.7 Component Selection

Suspendisse vel felis. Ut lorem lorem, interdum eu, tincidunt sit amet, laoreet vitae, arcu. Aenean faucibus pede eu ante. Praesent enim elit, rutrum at, molestie non, nonummy vel, nisl. Ut lectus eros, malesuada sit amet, fermentum eu, sodales cursus, magna. Donec eu purus. Quisque vehicula, urna sed ultricies auctor, pede lorem egestas dui, et convallis elit erat sed nulla. Donec luctus. Curabitur et nunc. Aliquam dolor odio, commodo pretium, ultricies non, pharetra in, velit. Integer arcu est, nonummy in, fermentum faucibus, egestas vel, odio. maybe talk about component selection for if it is the same size as the steering reeling mechanism

5.8 Summary

talk about how the design compromised on certain elements due to the scope of the project talk about desired implementations for increased functionality Suspendisse vel felis. Ut lorem lorem, interdum eu, tincidunt sit amet, laoreet vitae, arcu. Aenean faucibus pede eu ante. Praesent enim elit, rutrum at, molestie non, nonummy vel, nisl. Ut lectus eros, malesuada sit amet, fermentum eu, sodales cursus, magna. Donec eu purus. Quisque vehicula, urna sed ultricies auctor, pede lorem egestas dui, et convallis elit erat sed nulla. Donec luctus. Curabitur et nunc. Aliquam dolor odio, commodo pretium, ultricies non, pharetra in, velit. Integer arcu est, nonummy in, fermentum faucibus, egestas vel, odio.

6 Results

6.1 Introduction

Suspendisse vel felis. Ut lorem lorem, interdum eu, tincidunt sit amet, laoreet vitae, arcu. Aenean faucibus pede eu ante. Praesent enim elit, rutrum at, molestie non, nonummy vel, nisl. Ut lectus eros, malesuada sit amet, fermentum eu, sodales cursus, magna. Donec eu purus. Quisque vehicula, urna sed ultricies auctor, pede lorem egestas dui, et convallis elit erat sed nulla. Donec luctus. Curabitur et nunc. Aliquam dolor odio, commodo pretium, ultricies non, pharetra in, velit. Integer arcu est, nonummy in, fermentum faucibus, egestas vel, odio.

6.2 Methodology

Simulation Objectives and Scope: The methodology chosen for the simulation aims to evaluate the performance of the proposed hybrid-vine robot against other vine robot designs. **System Architecture and Block Diagram:** The model uses Simulink [28] to simulate the eversion of the vine robot. In addition to joint position MATLAB [29] which is then used to implement the kinematic model of the robot and aids in data display. **Robot Models and Assumptions:** The robot models that are simulated include different characteristic models relating to different robots. **Simulation Environment and Scenarios:** There are many simulation parameters such as joint parameters, timestep, materials parameters.

6.3 Path Length Dependency

Through previous vine robot modelling work [26] we obtain equations to describe yield pressure and tip velocity of the vine robot. Adapting these formulations to suit our proposed models we obtain,

$$PA = YA + \left(\frac{1}{\varphi} v \right)^{\frac{1}{n}} A \quad (18)$$

$$v = \varphi(P - Y)^n \quad (19)$$

Path Dependent terms for a vine robot

$$\mu_s w L + \sum_i C e^{\frac{\mu_c L_i}{R_i}} \quad (20)$$

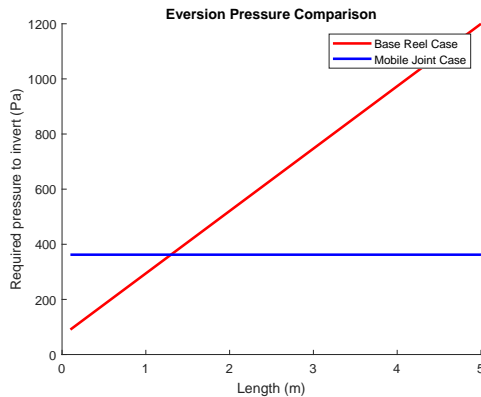


Fig. 19. Path Length Dependency of Proposed Vine Robot and Base Reeling Vine Robot

Observing Figure 19 shows eversion pressure for mobile joint system remains constant independent of length. This is due to the mobile joints of the vine robot preventing the inner sheath from

dragging along the base of the vine body. Additionally observing the eversion pressure of the base reeled vine robot initially outperforms the mobile joint system at distances below 1.2m but due to the linear nature due to the length dependent friction term, if we were to compare the mobile joint system to the steering-reeling mechanism in [22] they would exhibit the same constant behaviour with the mobile joint system eversion pressure being slightly higher due to the additional number of components and functionality adding to the weight of the joint and thereby increasing the friction force in contact with the outer sheath wall.

6.4 Path Bend Dependency

The proposed system is limited by the number of joints it possesses. The system will be outperformed by the internal steering-reeling mechanism proposed in [22], as when the number of bends in a tortuous path exceeds the number of joints this introduces capstan friction into the vine body due to inner sheath coming into contact with the outer sheath wall. However, it still outperforms base reel vine robots.

The system would perform well in predefined scenarios such as industrial maintenance where the workspace is known and the number of required joints to reach the desired locations in the workspace can be calculated.

6.5 System simulator

To model the movement of the mobile joint system inside the workspace, a dynamic simulator was developed to plot the shape of the vine robot body to visually show the space it occupies in the workspace.

6.5.1 Simulator

To model the movement of the mobile joint system inside the workspace, a dynamic simulator was developed to plot the shape of the vine robot body to visually show the how it's shape changes in the workspace. This simulator was developed in matlab app design, interpreting the real-time values of signals of a simulink model to replicate the length & shape change of the proposed mobile joint vine robot. This simulation makes the same assumptions for our kinematic model in Section

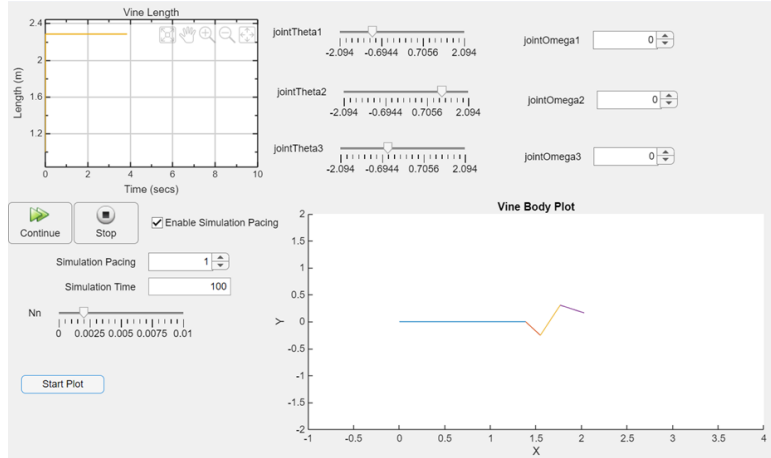


Fig. 20. Path Length Dependency of Proposed Vine Robot and Base Reeling Vine Robot

[4.8] The simulation allows for changes in simulation pacing and real-time plotting of the vine robot configuration as well as changing bend angle and linear speed of the mobile joints.

6.6 Summary

Mobile joint system outperforms base reeling vine robot in terms of length dependency & bend dependency with performance decreasing once no of bends exceeds the no of joints mobile joint system has similar performance to design in [22] but is outperformed on tortuous paths where capstan friction is introduced into the mobile joint system. A dynamic simulator was also developed to observe mobile joint system behaviour in real time by implementing a kinematics model and simulating tip speed.

7 Discussion

The mobile joint system would not be well suited to the tortuous environment of collapsed rubble, as internal friction increases exponentially once the total link bend exceeds the number of joints. However, the system could still prove useful in certain disaster sites or hazardous environment where the workspace is not crowded but is not suitable for human exploration. The model improves on base reeling vine robots in most situations, enhancing the shape control of vine robots. But fails to outperform the internal steering-reeling mechanism designed in [22] on tortuous paths. However, the inclusion of shape locking makes the proposed robot highly suitable for exploration of unstable structures due to its compliance and pose control. The scope of the project limited the amount of research that could be done into the proposed model, as experimental validation was not possible

in the scope of the project length and budget due to the project complexity. There were also organisational issues during the project, causing a change in supervisor with a specialty less relevant to robotics, despite this some meaningful results were still obtained. The system would perform well in predefined scenarios like industrial maintenance, where the workspace is known and the number of required joints to reach the desired locations in the workspace can be calculated

8 Conclusion

A novel vine robot actuation method has been presented that allows for shape locking & path-length independent operation as long as the soft link bendage is kept to a minimum during operation. Enhancing vine robot operation in unstable structures.

References

- [1] S. T. Robin R. Murphy and A. Kleiner, “Disaster robotics,” in *Springer Handbook of Robotics*, Berlin, Heidelberg: Springer, 2016, pp. 1577–1604. DOI: 10.1007/978-3-319-32552-1_60. [Online]. Available: https://link.springer.com/chapter/10.1007/978-3-319-32552-1_60 (cited on pp. 11, 14, 24).
- [2] W. Commons, *File:fsk rescue albania 2019.jpg — wikimedia commons, the free media repository*, [Online; accessed 17-April-2025], 2022. [Online]. Available: https://commons.wikimedia.org/w/index.php?title=File:FSK_Rescue_Albania_2019.jpg&oldid=667774605 (cited on p. 11).
- [3] W. Commons, *File:robots used during the chernobyl cleanup (11384369646).jpg — wikimedia commons, the free media repository*, [Online; accessed 17-April-2025; Licensed under CC BY-SA 4.0. <https://creativecommons.org/licenses/by-sa/2.0/deed.en>, 2024. [Online]. Available: [https://commons.wikimedia.org/w/index.php?title=File:Robots_used_during_the_Chernobyl_cleanup_\(11384369646\).jpg&oldid=975752251](https://commons.wikimedia.org/w/index.php?title=File:Robots_used_during_the_Chernobyl_cleanup_(11384369646).jpg&oldid=975752251) (cited on p. 15).
- [4] R. R. Murphy, S. Tadokoro, and A. Kleiner, “Disaster robotics,” in *Springer Handbook of Robotics*, 2nd Ed., 2014. [Online]. Available: <https://api.semanticscholar.org/CorpusID:31849866> (cited on p. 15).

- [5] M. Arai *et al.*, ““development of ‘souryu-iv’ and ‘souryu-v:’ serially connected crawler vehicles for in-rubble searching operations”,” *Journal of Field Robotics*, vol. 25, pp. 31–65, 2008. doi: 10.1002/rob.20229. [Online]. Available: <https://onlinelibrary.wiley.com/doi/10.1002/rob.20229> (cited on pp. 15, 16).
- [6] K. Osuka and H. Kitajima, “Development of mobile inspection robot for rescue activities: Moira,” in *Proceedings 2003 IEEE/RSJ International Conference on Intelligent Robots and Systems (IROS 2003) (Cat. No.03CH37453)*, vol. 4, 2003, 3373–3377 vol.3. doi: 10.1109/IROS.2003.1249677 (cited on pp. 15, 16).
- [7] R. Stopforth and G. Bright, “Required improvements and possible solutions for urban search and rescue (usar) robots.” in *ARCS*, 2008, pp. 53–57 (cited on p. 15).
- [8] W. Commons, *File:rescue robot tests to offer responders high-tech help (5940525341).jpg* — *wikimedia commons, the free media repository*, [Online; accessed 17-April-2025], 2024. [Online]. Available: [https://commons.wikimedia.org/w/index.php?title=File:Rescue_Robot_Tests_To_Offer_Responders_High-Tech_Help_\(5940525341\).jpg&oldid=888737965](https://commons.wikimedia.org/w/index.php?title=File:Rescue_Robot_Tests_To_Offer_Responders_High-Tech_Help_(5940525341).jpg&oldid=888737965) (cited on p. 16).
- [9] R. Murphy and S. Stover, “Rescue robots for mudslides: A descriptive study of the 2005 la conchita mudslide response,” *J. Field Robotics*, vol. 25, pp. 3–16, Feb. 2008. doi: 10.1002/rob.20207 (cited on p. 15).
- [10] K. Nagatani *et al.*, “Redesign of rescue mobile robot quince,” in *2011 IEEE International Symposium on Safety, Security, and Rescue Robotics*, 2011, pp. 13–18. doi: 10.1109/SSRR.2011.6106794 (cited on p. 15).
- [11] G. Baker *et al.*, “Atlas - urban search and rescue robot,” University of Warwick, Tech. Rep., 2017. [Online]. Available: https://warwick.ac.uk/fac/sci/eng/meng/wmr/projects/rescue/reports/1617reports/wmr_technical_report_2016-17.pdf (cited on p. 15).
- [12] J. Whitman *et al.*, “Snake robot urban search after the 2017 mexico city earthquake,” in *2018 IEEE International Symposium on Safety, Security, and Rescue Robotics (SSRR)*, 2018, pp. 1–6. doi: 10.1109/SSRR.2018.8468633 (cited on p. 16).
- [13] P. Chavan *et al.*, “Modular snake robot with mapping and navigation: Urban search and rescue (usar) robot,” in *2015 International Conference on Computing Communication Control and Automation*, 2015, pp. 537–541. doi: 10.1109/ICCCBEA.2015.110 (cited on p. 16).

- [14] W. Commons, *File:snakebot3.jpg — wikimedia commons, the free media repository*, [Online; accessed 17-April-2025], 2024. [Online]. Available: <https://commons.wikimedia.org/w/index.php?title=File:SnakeBot3.jpg&oldid=911225967> (cited on p. 17).
- [15] U. Jeong *et al.*, “Reliability analysis of a tendon-driven actuation for soft robots,” *The International Journal of Robotics Research*, vol. 40, no. 1, pp. 494–511, 2021. doi: 10.1177/0278364920907151. eprint: <https://doi.org/10.1177/0278364920907151>. [Online]. Available: <https://doi.org/10.1177/0278364920907151> (cited on p. 17).
- [16] A. Kitagawa, H. Tsukagoshi, and M. Igarashi, “Development of small diameter active hose-ii for search and life-prolongation of victims under debris,” *Journal of Robotics and Mechatronics*, vol. 15, no. 5, pp. 474–481, 2003. doi: 10.20965/jrm.2003.p0474 (cited on p. 17).
- [17] Y. Tang *et al.*, “Leveraging elastic instabilities for amplified performance: Spine-inspired high-speed and high-force soft robots,” *Science Advances*, vol. 6, no. 19, eaaz6912, 2020. doi: 10.1126/sciadv.aaz6912. eprint: <https://www.science.org/doi/pdf/10.1126/sciadv.aaz6912>. [Online]. Available: <https://www.science.org/doi/abs/10.1126/sciadv.aaz6912> (cited on p. 18).
- [18] M. D. Grissom *et al.*, “Design and experimental testing of the OctArm soft robot manipulator,” in *Unmanned Systems Technology VIII*, G. R. Gerhart, C. M. Shoemaker, and D. W. Gage, Eds., International Society for Optics and Photonics, vol. 6230, SPIE, 2006, 62301F. doi: 10.1117/12.665321. [Online]. Available: <https://doi.org/10.1117/12.665321> (cited on p. 18).
- [19] C. McFarland *et al.*, *Field insights for portable vine robots in urban search and rescue*, 2024. arXiv: 2411.06615 [cs.R0]. [Online]. Available: <https://arxiv.org/abs/2411.06615> (cited on p. 19).
- [20] M. M. Coad *et al.*, “Retraction of soft growing robots without buckling,” *IEEE Robotics and Automation Letters*, vol. 5, no. 2, pp. 2115–2122, Apr. 2020, ISSN: 2377-3774. doi: 10.1109/LRA.2020.2970629. [Online]. Available: <http://dx.doi.org/10.1109/LRA.2020.2970629> (cited on pp. 19, 20, 26, 32).
- [21] P. A. der Maur *et al.*, “Roboa: Construction and evaluation of a steerable vine robot for search and rescue applications,” in *2021 IEEE 4th International Conference on Soft Robotics (RoboSoft)*, 2021, pp. 15–20. doi: 10.1109/RoboSoft51838.2021.9479192 (cited on p. 20).

- [22] D. A. Haggerty, N. D. Naclerio, and E. W. Hawkes, “Hybrid vine robot with internal steering-reeling mechanism enhances system-level capabilities,” *IEEE Robotics and Automation Letters*, vol. 6, no. 3, pp. 5437–5444, 2021. doi: 10.1109/LRA.2021.3072858 (cited on pp. 20, 26, 29, 30, 40, 43, 44).
- [23] F. Taubner *et al.*, *Proboscis search and rescue - worm-like softrobot for search and rescue missions*, Jun. 2018 (cited on p. 22).
- [24] J. of Chemical Education, “Derivation of the ideal gas law,” *Journal of Chemical Education*, vol. 84, no. 11, p. 1832, 2007. doi: 10.1021/ed084p1832 (cited on p. 30).
- [25] V. L. Popov, “Coulomb’s law of friction,” in *Contact Mechanics and Friction: Physical Principles and Applications*. Berlin, Heidelberg: Springer Berlin Heidelberg, 2010, pp. 133–154, ISBN: 978-3-642-10803-7. doi: 10.1007/978-3-642-10803-7_10. [Online]. Available: https://doi.org/10.1007/978-3-642-10803-7_10 (cited on p. 31).
- [26] L. H. Blumenschein, A. M. Okamura, and E. W. Hawkes, “Modeling of bioinspired apical extension in a soft robot,” in *Proc. Conf. Biomimetic Biohybrid Syst.*, 2017, pp. 522–531 (cited on pp. 32, 42).
- [27] R. Williams and B. H. Shelley, “Inverse kinematics for planar parallel manipulators,” in *Proc. ASME Des. Tech. Conf.*, 1997, pp. 14–17 (cited on p. 33).
- [28] T. M. Inc., *Simulink version: 24.2 (r2024b)*, Natick, Massachusetts, United States, 2024. [Online]. Available: <https://www.mathworks.com/products/simulink.html> (cited on p. 42).
- [29] T. M. Inc., *Matlab version: 24.2 (r2024b)*, Natick, Massachusetts, United States, 2024. [Online]. Available: <https://www.mathworks.com> (cited on p. 42).

Appendices

A Project outline

Soft robot for navigation of confined rubble and small voids

Background

During natural disasters, such as earthquakes, landslides or tsunamis, urban search and rescue is a vital response to minimise the death toll from these events.

In the case of earthquakes this involves surveying and excavating the rubble of collapsed buildings, to locate and safely extract survivors.

Environment

These environments are generally non-uniform and potentially unstable confined spaces filled with rubble and debris, with much of this debris being sharp materials like broken glass, rock & exposed metal.

Survivors not found in the initial stages of rapid search and rescue are generally trapped in void spaces within the rubble of varying size. Due to the lack of ventilation of some of these spaces, survivors can suffocate due to buildup of carbon dioxide.

Motivation for project

The motivation for this project is to use the conformity of soft robotic joints to locate trapped survivors in small voids of collapsed buildings, that weren't extracted during the initial rapid search and rescue, and to provide a lifeline for these survivors until extraction.

Overall aim

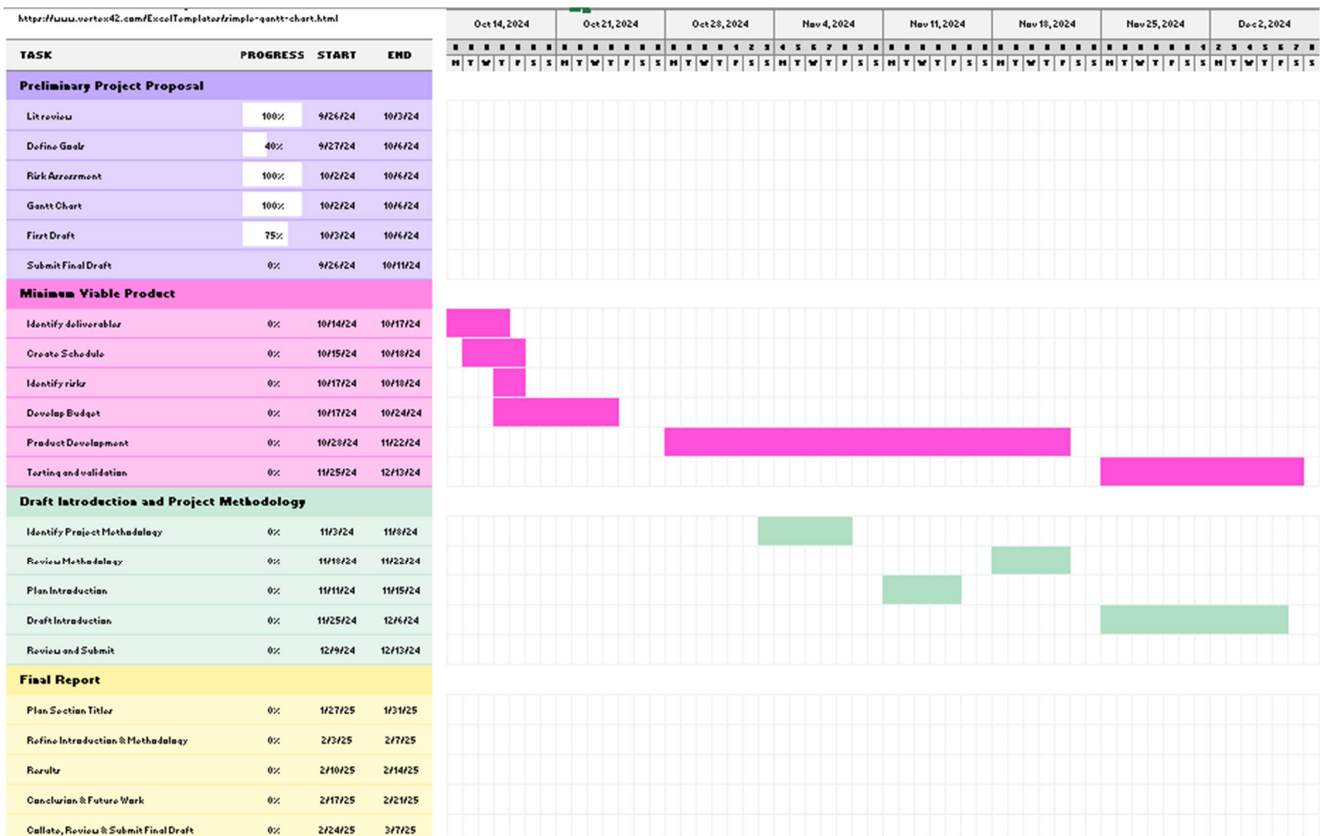
To produce a flexible soft robot that is capable of navigating through confined rubble

Milestones

- The robot shall fit through 50mm diameter holes [ref]
- The robot shall be portable
- The robot must be puncture resistant
- The robot shall move both horizontally and vertically
- The robot will be capable of relaying its surroundings at the end effector
- The robot shall be capable of fluid exchange from source to destination

Continued Professional Development Plan

- Gain knowledge of suitable soft robotic actuators
- Gain knowledge of simulation software for soft robotics



B Risk assessment



The University of Manchester

RISK REGISTER FOR 3rd YEAR PROJECT

Project Title:	Soft Robot For Confined Spaces		Submission Date:	10/10/2024	
Student Name:	Vincent	Vanhegan			

C Code

<https://github.com/DUDE44850/MobileJointVineRobotSim.git> The repository in the provided link includes a simulink model and a associated matlab APP which uses the data from the simulink simulation to simulate the kinematics of the proposed vine robot in this paper